Journal of Materials Chemistry A

Accepted Manuscript

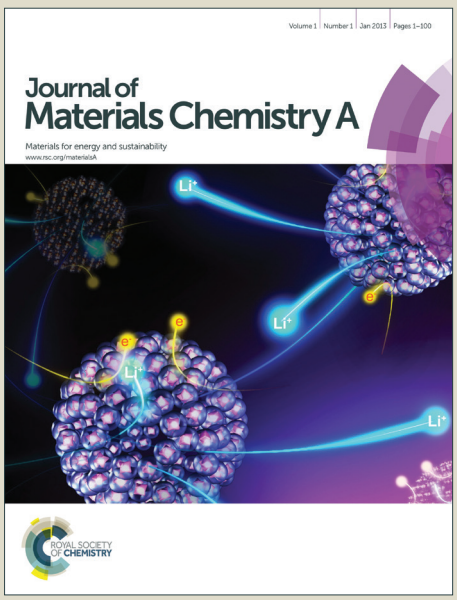

ROYAL SOCIETY OF CHEMISTRY

www.rsc.org/materialsA

Cite this: DOI: 10.1039/c0xx00000x

www.rsc.org/xxxxxx

ARTICLE TYPE

A new magnetic nanocomposite for selective detection and removal of trace copper ions from water

Xun Qiu [a], Najun Li* [a,b], Shun Yang [a], Dongyun Chen [a], Qingfeng Xu [a,b], Hua Li [a,b] and Jianmei Lu* [a,b]

Received (in XXX, XXX) Xth XXXXXXXXX 20XX, Accepted Xth XXXXXXXXX 20XX

DOI: 10.1039/b000000x

A core-shell structured magnetic nanocomposite (SDMA) modified by one kind of new organic fluorescent probe and selective chelating groups was prepared for simultaneous detection and removal of low concentration of Cu^{2+}. Series of experiments were designed to detect and adsorb copper ions in aqueous solution by SDMA. The results showed that SDMA could detect Cu^{2+} from copper ion solution qualitatively and quantificationally with a certain degree of selectivity, and remove Cu^{2+} with a respectable removal efficiency of about 80%. Through the contrast adsorption experiments, the adsorption capacity of SDMA was significantly higher than that of other two common magnetic nano adsorbents (Fe_3O_4@mSiO_2-SH and Fe_3O_4@mSiO_2-NH_2). The adsorption behavior of SDMA was studied through equilibrium and kinetic experiments. The adsorption isotherm was well fitted by Freundlich model perfectly and the pseudo-second-order model could fit the kinetic adsorption. Moreover, SDMA could reach the adsorption equilibrium in only 20 min, which showed a fast kinetic adsorption to Cu^{2+}. From the results of our completed work, it can be summarized that the prepared SDMA can be an effective and potential nano-adsorbent for detecting and removing copper ions from copper ions-containing wastewater.

Introduction

Copper ion, a metal ion indispensable for human beings, is the third most abundant transition metal elements in human body.[1] While according to the Word Health Organization (WHO), copper ions are indentified as hazardous pollutants in water.[2] Excessive exposure to copper will lead to the central nervous system disorders and physical health problems, such as Wilson's disease and Menkes' disease.[3] So the separation of copper ions from wastewater is highly valued, especially at low concentration.

Due to the jeopardy of potentially toxic metal ions in environment and biological systems, many approaches and materials have been studied to detect them.[4-7] For selective sensing and monitoring low concentration of potentially toxic metal ions, fluorescent probes techniques have been applied widely in biological samples because of their high sensitivity and simplicity.[8, 9] Compared with the traditional instrumental elemental analysis methods, such as atomic absorption spectroscopy (AAS) and coupled plasma mass spectrometry (ICP-MS), techniques of fluorescent probes are more flexible, convenient and timely.[10-13]

To remove the potentially toxic metal ions from contaminated water, a wide range of ways are employed, including adsorption, precipitation, and electrochemical removal, etc.[14-17] Among them, adsorption is the most prevailing beacuse it is a economical, conventional and efficient way.[18-20] Common adsorbents like silica, ion exchanger resins and activated carbon have been utilized in adsorption processes.[21-23] However these sorbents are usually cannot adsorb trace concentration of contaminants, or show poor adsorption capacity, efficiency and adsorption time. In recent years, selective adsorption materials for heavy metal ions have gained a growing interest.[24-27] According to reports,[28-30] many special magnetic nano-adsorbents for potentially toxic metal ions removal have been fabricated. But most of these magnetic nanomaterials for adsorption have no selectivity to special metal ions.

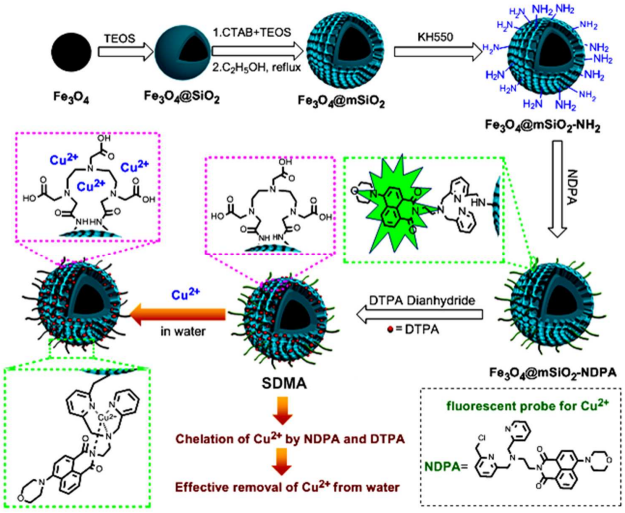

Scheme 1 Illustration of the synthetic procedure of SDMA and removal property of adsorbent for Cu^{2+}

Herein, a core-shell structured magnetic nanocomposite for preferential detection and efficient removal of trace copper ions from water is fabricated as a new nano-adsorbent (SDMA). Fe_3O_4 nanoparticles were used as the "core" because of its good magnetic separation manipulability and biocompatibility.[31] The shell of SDMA was mesoporous silica (mSiO_2),[32, 33] whose

surface was functionalized with plenty of amino groups. In addition, some modification was performed on the active amino groups. Firstly, a small amount of these amino groups were grafted by N-(di-2-picolylamine)-4-morpholinyl naphthalimide (NDPA, **Scheme 1**) that is an organic fluorescent probe showing high selectivity to copper ions.[34] Secondly, the large numbers of residual amino groups were grafted with diethylenetriaminepentaacetic (DTPA) that can provide numerous carboxyl groups and nitrogen atoms to chelate copper ions effectively.[35-37] Due to the NDPA, DTPA and the abundant nitrogen atoms of amino groups modified on the surface of $mSiO_2$, the functionalized magnetic nanocomposite showed high selectivity and sensitivity in detection of Cu^{2+} and then adsorption with much improved capacity. Furthermore, it can be separated from water with chelated Cu^{2+} under magnetization. The prepared magnetic nanoparticles were characterized, and selective detection and adsorption were studied and discussed in detail.

Experimental Section

Reagents

All the chemical agents used for the synthesis of SDMA in the experiment were purchased from the National Medicine Group Chemical Reagents Co., Ltd. Diethylenetriaminepentaacetic acid dianhydride (DTPA dianhydride) and the reagents used for synthesis of NDPA were of analytical grade and used without further purification. Anhydrous cupric sulfate was of analytical grade and used to provide copper ions in this study. Water used in the adsorption experiment was double distilled water.

Synthesis of Fe_3O_4@$mSiO_2$ microspheres

The magnetic Fe_3O_4 nanoparticles were prepared according to the literature.[38] In brief, 3.38 g $FeCl_3 \cdot 6H_2O$ and 9.00 g sodium acetate were dissolved in the solution of 1.25 g polyethylene glycol (PEG10000) in 100 mL ethylene glycol (EG) under stirring. After stirred for 20 min, the homogeneous yellow solution was transferred to the stainless-steel autoclave and heated at 200 □ for 8 h. Then the autoclave was cooled to room temperature. The black products were washed with ethanol several times, and dried in vacuum at 60 □ for 8 h.

The Fe_3O_4@$mSiO_2$ microspheres were prepared through the Stöber method.[39] Typically, 0.4 g of the prepared Fe_3O_4 particles were treated with 0.1 M HCl aqueous solution by ultr-asonication for 20 min. Then, the Fe_3O_4 nanoparticles were washed with deionized water, and dispersed in the mixture of 140mL ethanol, 60 mL deionized water and 1.5mL concentrated ammonia aqueous solution (28%). After, 0.12 mL tetraethyl orthosilicate (TEOS) was added dropwise with vigorous stirring at room temperature. The reaction lasted for 24 h, the obtained spheres were washed with ethanol and deionized water to remove the extra reactants, and then re-dispersed in a solution containing 350 mg cetyltrimethylammonium bromide (CTAB), 70 mL ethanol, 70 mL deionized water and 1.2 mL concentrated ammonia aqueous solution (28%). The mixture was homogenized under ultrasonication for 15 min, and stirred for another 15 min afterwards. Then 0.40 mL TEOS was added dropwise into the solution under vigorous stirring for 6 h. The product was collected by magnetic separation and repeatedly washed with ethanol and deionized water. The structure-directing agent CTAB was thereafter removed with ethanol reflux at 85 □. The products were separated and washed, then dried in vacuum at 60 □ overnight and placed in a desiccator before use.

Synthesis of Fe_3O_4@$mSiO_2$-NH_2 particles

To decorate the silica surface with amino groups, 2.5 mL 3-(aminopropyl) triethoxysilane (KH550) was added to the mixture containing 200 mg of Fe_3O_4@$mSiO_2$ and 150 mL toluene. Then stirred for 24 h, after this reaction, the magnetic nanoparticles were centrifuged and further washed with ethanol and deionized water. The produced microspheres were designated as Fe_3O_4@$mSiO_2$-NH_2 magnetic nanoparticles. The contrastive experiment was carried out with Fe_3O_4@$mSiO_2$-SH prepared by the same route but the silane coupling agent was 3-mercaptopropyl trimethoxysilane (KH590).

Synthesis of Fe_3O_4@$mSiO_2$-NDPA spheres

The NDPA was synthetized by the method as the previous literature,[34] the detailed process of synthesis was in supplementary information. The prepared magnetic nanoparticles were dispersed in 100 mL acetonitrile with 60 mg NDPA, 400 mg anhydrous potassium carbonate and 30 mg potassium iodide were added to promote the reaction afterwards, the mixture was agitated and refluxed for 24 h. After that, the mixture was cooled to room temperature, and the product was separated using a magnet. Obtained magnetic microspheres were washed with ethanol and deionized water. Then, these particles were refluxed by Soxhlet extractor and absolute ethyl alcohol was used as extractor to wash and remove the residual raw materials. Finally, the product was dried in a vacuum at 60 □. These obtained nanospheres were denoted as Fe_3O_4@$mSiO_2$-NDPA.

Synthesis of SDMA

420 mg DTPA dianhydride and 0.15 mL triethylamine were dissolved in 20 mL dry N,N-dimethylformamide. Subsequently, the mixture was refluxed at 70 □ under Ar atmosphere. After that, homogeneous mixture of 200 mg Fe_3O_4@$mSiO_2$-NDPA dispersed in 15 mL dry N,N-dimethylformamide was slowly added from a dropping funnel over 2 h. Then, 5 mL water was added into the reaction mixture, the reaction was continued for 1 h. The magnetic nanoparticles were separated under magnetic field and washed with ethanol and deionized water for several times. Then these black products were dried in vacuum at 60 □ overnight. Finally, the SDMA nanocomposites were obtained.

The fabrication process of the SDMA nanocomposite and its detection and removal of copper ions is shown in **Scheme 1**.

Characterization of nanoparticles

Transmission electron microscopy (TEM, Hitachi H600) was used to observe the transformation of nano particles in the synthetic process and the size of nanomaterial, the surface morphologies of SDMA was examined by scanning electron microscope (SEM, Hitachi S-4800), fourier transform infrared

spectroscopy (FT-IR, Nicolet 4700) was employed to represent the consequence after wrapping SiO_2, The chemical composition of SDMA was determined by X-ray photoelectron spectra (XPS, Axis Ultra HAS). The magnetism of SDMA was test qualitatively by the action of an applied magnetic field.

Selective detection of SDMA for Cu^{2+}

Firstly, the fluorescence spectrum characteristic of NDPA was investigated. 1 mL of NDPA methanol solution (10 mmol/L) were added into 2 mL solutions of different concentrations of Cu^{2+} (0, 0.05, 0.10, 0.15, 0.25, 0.50, 1.00, 1.50, 2.50, 5.00, 10.00 mg/L) respectively to get the emission spectra of NDPA. Secondly, study on the selectivity of SDMA. 1mL of SDMA suspension (1mg/mL, in methanol) were added into 2mL different solutions of metal ions (100μmol/L, Mn^{2+}, Fe^{3+}, Cr^{6+}, Zn^{2+}, Cu^{2+}, Ni^{2+}, Hg^{2+}, Pb^{2+}) respectively to measure the emission spectra of SDMA. Thirdly, quantitative detection of Cu^{2+}. 1 mL of SDMA suspension (1 mg/mL, in methanol) were added into 2 mL solutions of different concentrations of Cu^{2+} (0, 1.5, 2.5, 3.5, 4.5, 5.5, 6.5, 7.5 mg/L) respectively to get the emission spectra of SDMA.

The studies on selective detection of Cu^{2+} were conducted with three times respectively and standard deviations were calculated.

Adsorption experiments

Batches of experiments were carried out to investigate the Cu^{2+} adsorption performances. In the static equilibrium adsorption experiments, 3 mg of different nanoadsorbents (SDMA, Fe_3O_4@mSiO_2-NH_2 and Fe_3O_4@mSiO_2-SH) were respectively added into 10 mL of Cu^{2+} solutions which were prepared in various initial concentrations (1.5, 3.5, 5.5, 6.5, 7.5, 10.0, 15.0 mg/L). Then, shaken at 20 □ for 5 h. The concentrations of these final solutions were analyzed by UV-Vis spectrophotometry. The adsorption capacities (Q_e) of adsorbents were determined using the following equation:

$$Q_e=(C_0-C_e)V/W \qquad (1)$$

where Q_e (mg/g) represents the adsorption capacities of SDMA, Fe_3O_4@mSiO_2-NH_2 and Fe_3O_4@mSiO_2-SH towards copper ions, C_0 and C_e (mg/L) are the initial and equilibrium concentration of Cu^{2+}, V (mL) denoted the volume of solution, W (g) is the weight of the adsorbents.

In the dynamic adsorption experiments, 10 mL of the copper ions solutions at different concentrations (2.5 mg/L, 3.5 mg/L and 4.5 mg/L) were poured into bottles severally, then, 3 mg of SDMA were added respectively. The bottles were then placed in the shaker bath at 20 ℃. To measure the Cu^{2+} concentration at regular intervals until the reactions reach adsorption equilibrium and the concentrations change no longer. The amounts of Cu^{2+} adsorbed on SDMA were calculated.

In the selective adsorption experiments, 3 mg of SDMA were added into 5 mL of various metal ions solution with an initial concentration of 100 μmol/L. Subsequently, the solutions were shaken at 20 ℃ for 3 h to reach adsorption equilibrium. At last, atomic absorption spectroscopy was used to analyze the concentrations of metal ions.

The pH of the solution strongly affects adsorption capacity of adsorption materials. To investigate the influence, 3 mg SDMA was added into 5.5 mg/L copper ions solutions which at different pH values (4, 5, 6, 7, 8, 9, 10). Then, the solutions were placed in the shaker bath at 20 □ for 3 h to reach equilibrium. The equilibrium concentrations were analyzed by UV-Vis spectrophotometer and the amounts of copper ions adsorbed on SDMA were calculated.

Results and discussion

Characterization of SDMA

The micro-structure and morphology of magnetic nanoparticles were analyzed (**Fig. 1**). From **Fig. 1a**, the synthetic Fe_3O_4 with an average diameter about 400 nm with good dispersity. As shown in **Fig. 1b** and **Fig. 1c**, both Fe_3O_4@SiO_2 and Fe_3O_4@mSiO_2 are spherical and mesoporous silica layer was wrapped on the Fe_3O_4@SiO_2 with a thickness of about 100 nm. As the SEM image of SDMA (**Fig.1d**) shown, the magnetic nanocomposites modified by functional groups kept nanospherical. The FT-IR spectra of Fe_3O_4 and Fe_3O_4@mSiO_2 are displayed in **Fig.1e**. The peak observed at 580 cm^{-1} was characteristic of the Fe-O vibration.[40] After coating reaction, the peaks of 3425 cm^{-1} and 1089 cm^{-1} were found, which were derived from the stretching vibration of Si-OH and Si-O bonds, respectively.[30] The FT-IR spectra results further confirmed the uniform coating of silica shell. The dispersion and magnetic separation of SDMA were examined to analyze the magnetism qualitatively (**Fig.1f**). SDMA could disperse in water easily and steadily because of the effect of silica layer. Under the applied external magnetic field, magnetic microspheres are separated completely only within 10 seconds. It indicates that SDMA has favorable dispersibility and superior strong magnetism which are helpful for practical application.

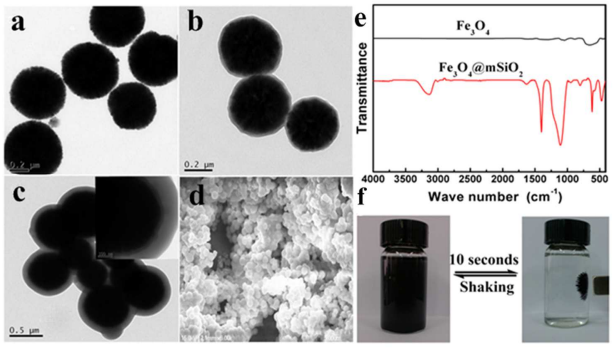

Fig.1 TEM images of Fe_3O_4 (a), Fe_3O_4@SiO_2 (b), Fe_3O_4@mSiO_2 (c); SEM image of SDMA (d); FT-IR spectra of Fe_3O_4 and Fe_3O_4@mSiO_2 (e); photo of the magnetic-redispersion process of SDMA (f).

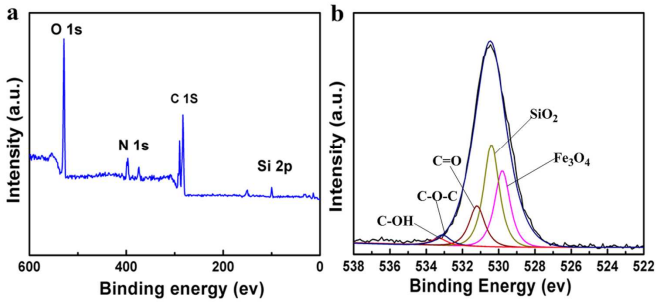

Fig. 2 Full range XPS spectra of SDMA (a); O1s XPS spectra of SDMA (b).

The modification of NDPA and DTPA with amino groups on Fe_3O_4@$mSiO_2$-NH_2 were confirmed by XPS spectra analysis. The XPS spectrum for key elements of SDMA are shown in **Fig.2a**. The results showed evidence for the existence of O, C, N and Si. Because of the graft of –NH_2 by silane coupling reaction, the DTPA and NDPA can be modified on the surface of $mSiO_2$, Hence, the presence of N in XPS spectrum of SDMA can indirectly prove that the amino groups are grafted on the surface of $mSiO_2$ successfully. **Fig.2b** is the O1s XPS spectrum of SDMA, which can be well fitted to five peaks at about 529.8 eV, 530.4 eV, 531.2 eV, 533.1 eV and 533.3 eV. They can be attributed to the binding energies of oxygen atoms bonded to Fe, Si, C in Fe_3O_4, SiO_2, C=O, C-O-C and C-OH, respectively. The C-O-C was in morpholine of NDPA and the C-OH was in carboxyl groups of DPTA. These results verified NDPA and DTPA were decorated on the surface of $mSiO_2$ smoothly.

Selective Detection of Copper Ions

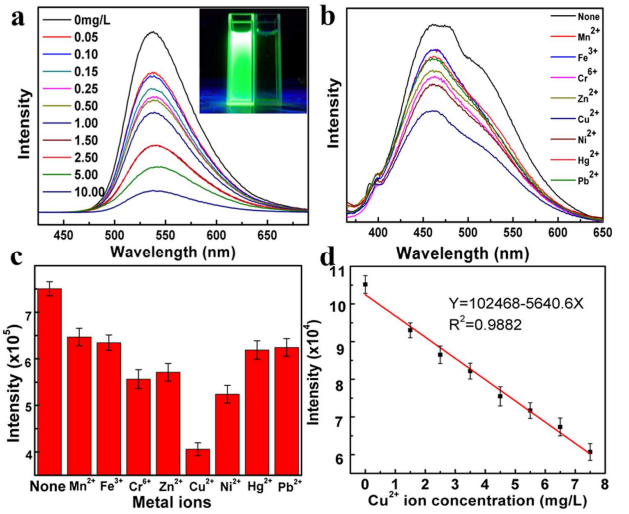

Fig.3 Fluorescence emission spectra of NDPA in the presence of increasing amounts of Cu^{2+} (a), the intensity was recorded at 550 nm, excitation at 350 nm. Inset: photograph of NDPA (left) and NDPA in the presence of excess amount of Cu^{2+} (right) under a 365 nm UV light; Fluorescence emission spectra of SDMA upon addition of different metal ions (b), the intensity was recorded at 460 nm, excitation at 350 nm; Bar graph of fluorescence intensity of SDMA at 460nm upon addition of different metal ions (c); The curve of fluorescence intensity at 460 nm vs. Cu^{2+} concentration (d).

Copper ions could give rise to fluorescence quenching of NDPA. As **Fig.3a** shown, NDPA reveals a fluorescence band centered at 550 nm under the excitation wavelength of 350 nm. After the addition of Cu^{2+} to the aqueous solution of NDPA, the fluorescence emission at 550 nm gradually reduced. Even the concentration of Cu^{2+} is only 0.05 mg/L, the change of fluorescence intensity is still distinct. it proves the detection limit is definite lower than 0.05 mg/L and it is extremely low for detecting Cu^{2+} from water. So NDPA could be used for well detection of trace amounts of copper ions. Due to the high recognition performance of NDPA to copper ions,[34] the selective detection of copper ions from other metal ions by SDMA was carried out, as the fluorescence emission spectra shown in **Fig.3b**. Keeping the same excitation wavelength at 350 nm, the fluorescence emission spectra of SDMA had a large blue shift with a peak at 460 nm due to the black core of Fe_3O_4. Furthermore, the addition of metal ions weakened the fluorescence intensity of SDMA, especially Cu^{2+}. Converted into a bar graph (**Fig. 3c**), it is more clear to find that copper ions could quench fluorescence of SDMA much more drastically than other metal ions. Based on **Fig.3b** and **Fig. 3c**, it can be concluded that SDMA could detect copper ions from water with high selectivity.

In order to further investigate the detection performance of SDMA for copper ions, fluorescence intensities of SDMA *vs* copper ions solutions at different concentrations were studied (**Fig.3d**). Combined with the results in **Fig.3d,** when the copper ion concentration is low, the fluorescence intensity (λ_{ex} = 460 nm) decreases with copper ions concentration in a good linear relationship (R^2 = 0.9882). As the obtained results, SDMA could detect the exact density of low concentration copper ion solution.

Adsorption of Copper Ions from Water

It is known that Fe_3O_4@$mSiO_2$-NH_2 and Fe_3O_4@$mSiO_2$-SH are two common nano-adsorbents for removing potentially toxic metal ions.[41-43] For comparing the adsorption capacity of SDMA with that of the other two adsobents, the adsorption isotherms at 20 ℃ were investigated. As **Fig.4a** shown, the Cu^{2+} adsorption capacity on SDMA reached about 27.5 mg/g, while the adsorption capacities on Fe_3O_4@$mSiO_2$-NH_2 and Fe_3O_4@$mSiO_2$-SH are much lower (about 16 mg/g and 22 mg/g, respectively).

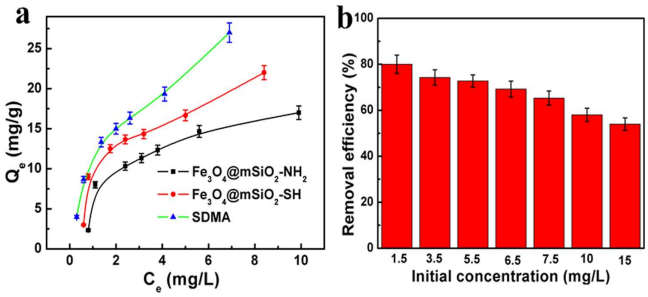

Fig.4 Adsorption isotherms of SDMA, Fe_3O_4@$mSiO_2$-SH and Fe_3O_4@$mSiO_2$-NH_2 (a); Removal efficiency of SDMA at different initial Cu^{2+} concentrations (b).

In our present work, the commonly familiar Langmuir and Freundlich models were used to fit the equilibrium isotherms for SDMA, the forms can be expressed as the following equations:

$$\text{Langmuir model}: C_e/Q_e = 1/K_L Q_m + C_e/Q_m \quad (2)$$

$$\text{Freundlich model}: \text{Log}Q_e = \log K_f + 1/n \log C_e \quad (3)$$

where C_e is the concentration of copper ions in solution at equilibrium (mg/L); Q_e is the adsorption capacity (mg/g); Q_m and K_f are constants in Langmuir and Freundlich model which are related to maximum adsorption capacity, repectively; K_L is a constant in Langmuir model which is related to the energy of adsorption; n is the Freundlich constant related to adsorption intensity.

Table 1 Langmuir and Freundlich isotherm parameters of copper ions onto SDMA

T(K)	Langmuir	Freundlich

293	Q_m(mg/g)	K_L(L/mg)	R^2	K_F	n	R^2
	35.71	0.36	0.96	9.09	1.68	0.98

The fitting isotherm parameters of the two models are listed in **Table 1**. Both the Langmuir and Freundlich models are suitable for describing the copper ions isotherm of SDMA, and the theoretical adsorbing capacity in Langmuir model is 35.71 mg/g. However, the higher value of regression coefficient (R^2) confirms that the Freundlich model could better fit the isotherm than Langmuir model. From the Freundlich model. It can be indicated that the adsorption process fitted the characteristics of multilayer and heterogeneous surface adsorption.[44] Moreover, the parameter n in Freundlich model is greater than 1, which indicated it was a favorable adsorption that means the intense adsorption behavior between adsorbent (SDMA) and adsorbate (Cu^{2+}).

Fig.4b reflect the Cu^{2+} removal efficiency of SDMA at different initial copper ions concentrations. It can be seen clearly that SDMA could adsorb trace of copper ions with a high removal efficiency. Typically, for 1.5 mg/L of copper-containing solution, the adsorption capacity is 4 mg/g and only 3 mg SDMA can remove 80% of Cu^{2+} from 10 mL of solution.

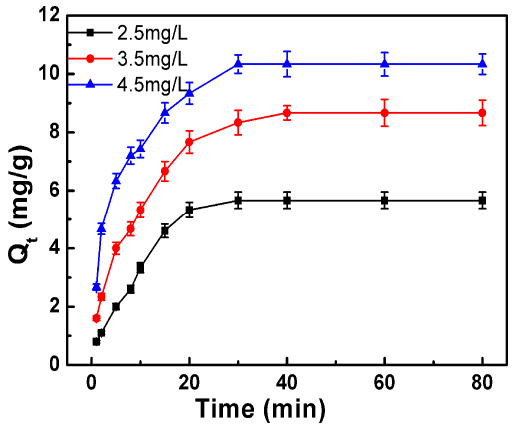

Fig. 5 Adsorption kinetic study for copper ions onto SDMA.

Adsorption kinetics is an essential parameter for investigating the removal rate. The adsorption kinetics of Cu^{2+} at various concentrations were studied in **Fig.5**. The adsorption rate at initial stage was fast and then became slow gradually until the equilibrium after about 20 min. In order to analyze the adsorption kinetic mechanism, the obtained kinetic data was fitted with pseudo-first-order and pseudo-second-order kinetic models, respectively. The two models can be written as the follows:

$$\text{pseudo-first-order}: \quad q_t = qe\cdot(1-\exp(-k_1\cdot t)) \qquad (4)$$

$$\text{pseudo-second-order}: \quad t/q_t = 1/(k_2 q_e^2) + t/q_e \qquad (5)$$

where q_t is the amount of Cu^{2+} adsorbed at time t (mg/g), q_e is the amount of Cu^{2+} adsorbed at equilibrium (mg/g); k_1(min^{-1}) and k_2(g/mg·min) are the rate constants of pseudo-first-order and pseudo-second-order kinetic models, respectively.

The adsorption kinetic parameters were summarized in **Table 2** and **Table 3**. As can be seen, the correlation coefficient (R^2) in pseudo-second-order model was closer to 1.0 than that in pseudo-first-order model. Consequently, it can be speculated that the adsorption kinetics fit better to the pseudo-second-order model than the pseudo-first-order model. That means the adsorption rate is dependent only on the adsorption capacity, but not the Cu^{2+} concentration, and it also indicates the adsorption of Cu^{2+} onto SDMA is based on the chemisorption controlled rate of the process.[44] Moreover, by comparison, the adsorption capacity of pseudo-second-order model is higher than that of pseudo-first-order model. Hence, SDMA shows a good adsorption capacity.

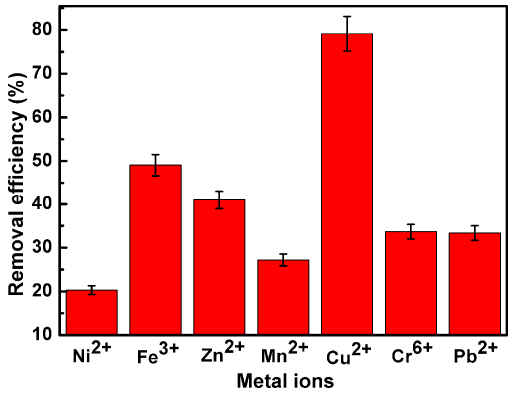

Fig. 6 Bar graph of the removal efficiency of 5 mL of 100 μmol/L different metal ions onto 3 mg SDMA.

Fig. 6 is the result of selective adsorption experiments. 3 mg SDMA can remove 100 μmol/L of 5 mL Cu^{2+} solution with a efficiency of 79.1%. Under the same molarity, the Cu^{2+} removal efficiency is distinct higher than others', especially the Ni^{2+} removal efficiency. So the selectivity of SDMA to Cu^{2+} is manifest.

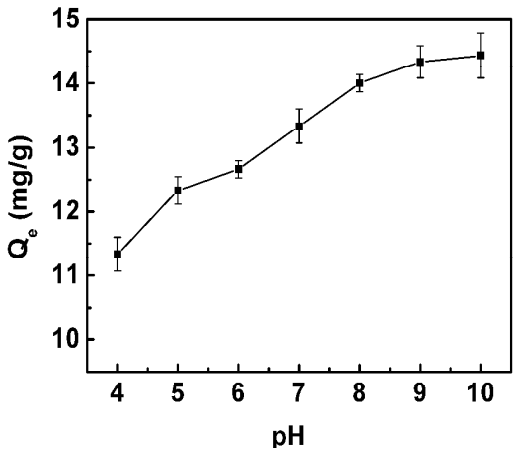

Fig. 7 Effect of pH on the copper ions removal capacities of SDMA

The pH of adsorption medium is one of the most important parameters affecting metal ions adsorption capacities.[45] **Fig.7** reflected the results of effect of pH values. The adsorption capacities were gradually increasing with the pH values increased. When pH values greater than 8, the adsorption capacities raised slowly and trend to a balanced numerical value. This reason of the expression owes to the increasingly deprotonated SiO_2-DTPA groups and above pH 9, the solubility product of Cu^{2+} is exceeded (2.2×10^{-20}) and the Cu^{2+} in solution precipitate as $Cu(OH)_2$.

Conclusions

A new core-shell structured spherical magnetic nanocomposite (SDMA) with a diameter of about 400 nm for simultaneous

detection and removal of low concentration of Cu^{2+} was prepared. SDMA exhibited super magnetic properties and good disperibility in water. Selectivity detection and adsorption experiments indicated that SDMA had high selectivity to detect and adsorb trace concentration of copper ions from water until 0.05 mg/L. In the equilibrium adsorption experiment, 3 mg SDMA could adsorb 10 mL 1.5 mg/L copper ions with a high removal efficiency of 80%. The adsorption capacity is much higher than that of same mass of Fe_3O_4@mSiO_2-SH and Fe_3O_4@mSiO_2-NH_2. Freundlich model can fit the adsorption isotherm perfectly and it indicates the adsorption was a multilayer and heterogeneous surface adsorption process with a strong adsorption intensity. In addition, SDMA could adsorb copper ions to reach equilibrium within 20 min, and the adsorption followed pseudo-second-order model well that means the adsorption rate was controlled by chemisorption. In summary, SDMA can be envisioned as an effective and potential nano-adsorbent for detection and removal of copper ions from copper-containing wastewater.

Table 2 Kinetics parameters of pseudo-first-order model for adsorption of copper ions based on SDMA.

C_o (mg/L)	Pseudo-first-order $q_t=qe\cdot(1-\exp(-k_1\cdot t))$	Q_{exp}(mg/g)	Q_{mod}(mg/g)	K_1(min^{-1})	R^2
2.5	q_t=5.8410· (1-exp(-0.0921·t))	5.667	5.8410	0.0921	0.982
3.5	q_t=8.6342· (1-exp(-0.0925·t))	8.667	8.6342	0.0925	0.952
4.5	q_t=9.3864· (1-exp(-0.2238·t))	9.667	9.3864	0.2238	0.939

Table 3 Kinetics parameters of pseudo-second-order model for adsorption of copper ions based on SDMA.

C_o (mg/L)	Pseudo-second-order $t/q_t=1/(k_2q_e^2)+t/q_e$	Q_{exp}(mg/g)	Q_{mod}(mg/g)	K_2(g/mg·min)	R^2
2.5	$t/q_t=0.1549t+1.2479$	5.667	6.4558	0.0240	0.988
3.5	$t/q_t=0.1037t+0.7604$	8.667	9.6432	0.0108	0.992
4.5	$t/q_t=0.099t+0.2605$	9.667	10.1010	0.0098	0.999

Acknowledgements

We gratefully acknowledge the financial support provided by National Natural Science Foundation of China (21336005, 21301125), National Science and Technology Pillar Program (2012BAC14B03), Natural Science Foundation of Jiangsu Province (BK2012625), Natural Science Foundation of the Jiangsu Higher Education Institutions of China (13KJB430022) and Suzhou Nano-project (ZXG201420).

Notes and references

[a] *College of Chemistry, Chemical Engineering and Materials Science,Collaborative Innovation Center of Suzhou Nano Science and Technology, Soochow University, Suzhou, 215123 China.*

[b] *State Key Laboratory of Treatments and Recycling for Organic Effluents by Adsorption in Petroleum and Chemical Industry, Suzhou, 215123 China.*

** E-mail: linajun@suda.edu.cn, lujm@suda.edu.cn; Tel./Fax: +86 (0) 512-6588 0367.*

† Electronic Supplementary Information (ESI) available: See DOI: 10.1039/b000000x/

1 X. Wang, X. Ma, Z. Yang, Z. Zhang, J. H. Wen, Z. R. Geng and Z. L. Wang, *Chem. Comm.*, 2013, **49**, 11263-11265.
2 S. Huang, C. Fan and C. Hou. *J. Hazad. Mater.*, 2014, **278**, 8-15.
3 K. J. Barnham, C. L. Masters and A. I. Bush, *Nat. Rev. Drug Discovery.*, 2004, **3**, 205-214.
4 K. P. Carter, A. M. Young and A. E. Palmer, *Chem. Rev.*, 2014, **114**, 4564-4601.
5 M. Katie, L. Enzo, A. J. Zhao and G. Chris, *Anal. Bioanal. Chem.*, 2012, **402**, 3263-3273.
6 J. S. Becker, M. Zoriy, A. Matusch, B. Wu, D. Salber, C. Palm and J. Susanne Becker, *Mass Spectrom. Rev.*, 2010, **29**, 156-175.
7 X. Qiu, S. Han, Y. Hu, M. Gao and H. Wang, *J. Mater. Chem. A.*, 2014, **2**, 1493-1501.
8 T. Gunnlaugsson, M. Glynn, G. M. Tocci, P. E. Kruger and F. M. Pfeffer, *Coord. Chem. Rev.*, 2006, **250**, 3094-3117.
9 W. Wang, X. Wang, Q. Yang, X. Fei, M. Sun and Y. Song, Chem. Commun., 2013, 49, 4833-4836.
10 T. Cheng, T. Wang, W. Zhu, X. Chen, Y. Yang, Y, Xu and X, Qian, *Org. Lett.*, 2011, **13**, 3656-3659.
11 E. M. Nolan and S. J. Lippard, *J. Am. Chem. Soc.*, 2007, **129**, 5910-5918.
12 E. M. Nolan and S. J. Lippard, *J. Am. Chem. Soc.*, 2003, **125**, 14270-14271.
13 H. S. Jung, M. Park, J. H. Han, J. H. Lee, C. Kang, J. H. Jung and J. S. Kim, *Chem. Commun.*, 2012, **48**, 5082-5084.
14 S. Singh, K. C. Brick and D. Bahadur, *J. Mater. Chem. A.*, 2013, **1**, 3325-3333.
15 Z. Wang, Y. Feng, X. Hao, W. Huang and X. Feng, *J. Mater. Chem. A.*, 2014, **2**, 10263-10272.
16 M. M. Matlock, B. S. Howerton and D. A. Atwood, *Water Res.*, 2002, **36**, 4757-4764.
17 A. Guijarro-Aldaco, V. Hern´andez-Montoya, A. Bonilla-Petriciolet, M. A. Montes-Mor´an and D. I. Mendoza-Castillo, *Ind. Eng. Chem. Res.*, 2011, 50, 9354-9362.
18 B. E. Reed, W. Lin, M. R. Matsumoto and J. N. Jensen, *Water Environ. Res.*, 1997, **69**, 444–461.
19 T. S. Sreeprasad, S. M. Maliyekkal, K. P. Lisha and T. Pradeep, *J. Hazard.Mater.*, 2011, **186**, 921-931.
20 W. S. Wan Ngah and M. A. K. M. Hanafiah, *Bioresour. Technol.*, 2008, **99**, 3935-3948.
21 D. Mohan, C. U. Pittman, *J. Hazard. Mater.*, 2006, 137, 762–811.
22 B. E. Reed and M. R. Matsumoto, *Sep. Sci. Technol.*, 1993, 28, 2179–2195.
23 E. Uğuzdoğan, E. B. Denkbaş and O. S. Kabasakal, *J. Hazard.Mater.*, 2010, **117**, 119-125.
24 G. Bayramoglu and M. Y. Arica, *J. Hazard.Mater.*, 2011, **187**, 213-221.

25 C. Kang, W. Li, L. Tan, H. Li, C. Wei and Y. Tang, *J. Mater. Chem. A.*, 2013, **1**, 7147-7153.
26 X. Luo, L. Liu, F. Deng and S. Luo, *J. Mater. Chem. A.*, 2013, **1**, 8280-8286.
27 M. Saraji and H. Yousefi, *J. Hazard.Mater.*, 2009, **167**, 1152-1157.
28 W. Zhang, X. Shi, Y. Zhang, W. Gu, B. Li and Y. Xian, *J. Mater. Chem. A.*, 2013, **1**, 1745-1753.
29 D. Dupont, W. Brullot, M. Bloemen, T. Verbiest and K. Binnemans, *ACS Appl. Mater. Interfaces.*, 2014, **6**, 4980-4988.
30 R. Yi, G. Ye, D. Pan, F. Wu, M. Wen and J. Chen, *J. Mater. Chem. A.*, 2014, **2**, 6840-6846.
31 M. Shao, F. Ning, J. Zhao, M. Wei, D.G. Evans and X. Duan, *J. Am. Chem. Soc.*, 2012, **134**, 1071-1077.
32 Z. Teng, C. Sun, X. Su, Y. Liu, Y. Tang, Y. Zhao, G. Chen, F. Yan, N. Yang, C. Wang and G. Lu, *J. Mater. Chem. B.*, 2013, **1**, 4684-4691.
33 C. Kresge, M. E. Leonowicz, W. J. Roth, J. C. Vartuli and J. S. Beck, *Nature*, 1992, **359**, 710-712.
34 X. Zhang, X. Jing, T. Liu, G. Han, H. Li and C. Duan, *Inorg. Chem.*, 2012, **51**, 2325-2331.
35 I. Pavlovic, M. R. Pérez, C. Barriga and M. A. Ulibarri, *Appl. Clay. Sci.*, 2009, **43**, 125-129.
36 J. Roosen and K. Binnermans, *J. Mater. Chem. A.*, 2014, **2**, 1530-1540.
37 C. H. Culberson, Y. J. Liang, T. M. Church and R. H. Wood, *Anal. Chim. Acta.*, 1982, **139**, 373-377.
38 P. Yang, Z. Quan, Z. Hou, C. Li, X. Kang, Z. Cheng and J. Lin, *Biomaterials*, 2009, **30**, 4786-4795.
39 W. Stöber, A. Fink and E. Bohn , *J. Colloid. Interface. Sci.*, 1958, **26**, 62-69.
40 S. Shi, J. Guo, Q. You, X. Chen and Y. Zhang, *Chem. Eng. J.*, 2014, **243**, 485-493.
41 X. Feng, G. E. Freyxell, L. Wang, A. Y. Kim, J. Liu and K. M. Kemner, *Science*, 1997, **276**, 923-926.
42 L. Mercier and T. J. Pinnavaia, *Adv. Mater.*, 1997, **9**, 500.
43 A. M. Liu, K. Hidajat, S. Kawi and D. Y. Zhao, *Chem. Commun.*, 2000, **13**, 1145-1146.
44 R. K. Sharma, A. Puri, Y. Monga and A. Adholeya, *J. Mater. Chem. A.*, 2014, **2**, 12888-12898.
45 D. Dupont, W. Brullot, M. Bloemen, T. Verbiest and K. Binnemans, *ACS Appl. Mater. Interfaces*, 2014, **6**, 4980–4988.

Graphical Abstract

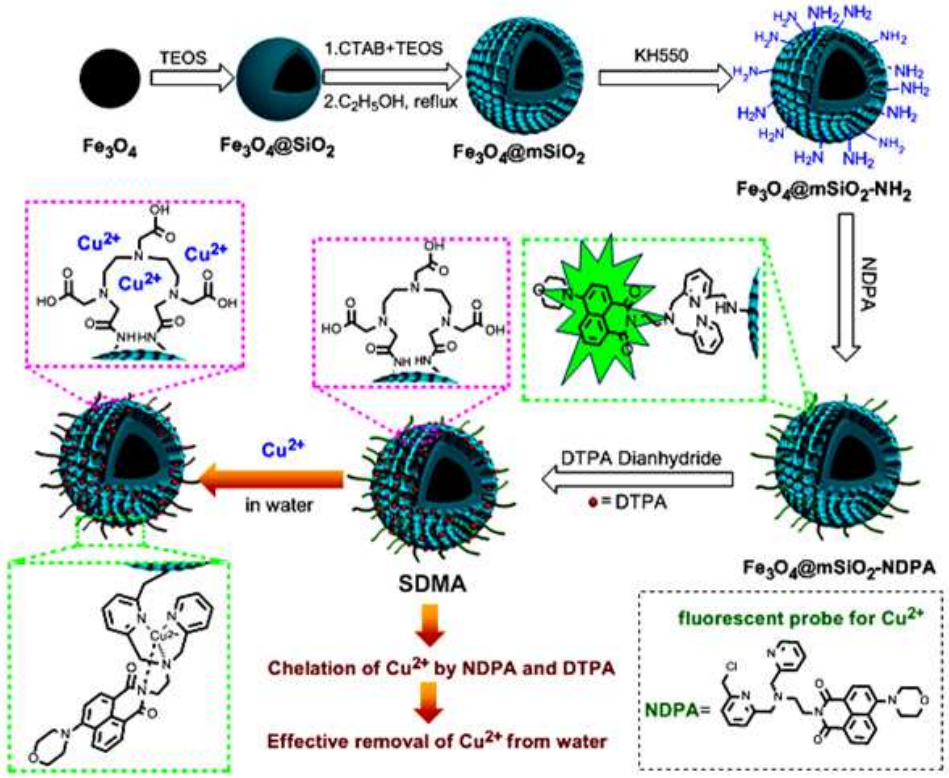

A new core-shell structured magnetic nanocomposite (SDMA) modified by one kind of new organic fluorescent probe and selective chelating groups was successfully prepared for simultaneous detection and removal of low concentration of Cu^{2+}. In this facile strategy, the new nanocomposites could detect trace of copper ions by the fluorescent probe modified on the surface of Fe_3O_4@$mSiO_2$, and adsorb Cu^{2+} from water with high capacity and good removal efficiency. Under the applied external magnetic field, SDMA could be separated from water very quickly.